Astron. Astrophys. 294, 155–164 (1995)

ASTRONOMY AND ASTROPHYSICS

Nonaxisymmetric dynamo solutions and extended starspots on late-type stars

David Moss[1], Dale M. Barker[2], Axel Brandenburg[3], and Ilkka Tuominen[4]

[1] Mathematics Department, The University, Manchester M13 9PL, UK
[2] Meteorological Office, London Rd, Bracknell, Berks RG12 2SZ, UK
[3] HAO/NCAR*, P.O Box 8000, Boulder, CO 80307, USA
[4] Observatory, P.O. Box 14, SF-00014 University of Helsinki, Finland

Received 5 April 1994 / Accepted 27 July 1994

Abstract. We have computed mean field dynamo models in a deep spherical shell, without restriction on spatial symmetries, in which the growth of the magnetic field is limited solely by the back reaction of the large scale Lorentz force on the large scale motions. A parameterization of the Reynolds stress tensor is included to describe the generation of differential rotation. We find for moderate values of the Taylor number, when the differential rotation is also small, that the stable magnetic fields are nonaxisymmetric, with the same basic topology as a 'perpendicular dipole'. For larger Taylor numbers, and stronger absolute differential rotation, we expect axisymmetric fields to be stable. We briefly discuss the relevance of our results to the large scale nonaxisymmetric structures and extended starspots observed on late type 'active giant' and other stars.

Key words: stars: magnetic fields – MHD – stars: activity

1. Introduction

Observational evidence has accumulated that nonaxisymmetric structures of global scale are present on the surfaces of active stars with deep outer convection zones, both giants (see, e.g., the discussion in Moss et al. 1991 and Jetsu et al. 1993) and dwarfs (e.g. Jetsu 1993). From analogy with the solar spots, it seems probable that there are corresponding global scale magnetic structures present, i.e. large scale nonaxisymmetric magnetic fields.

Active late-type stars show rotational modulation of their brightness, indicating surface inhomogeneities. Such surface inhomogeneities are usually associated with starspots, although their size distribution is probably rather different from the solar case. Surface temperature maps show that such cool starspots extend over as much as 20-30 degrees (e.g. Piskunov et al. 1990, 1994). The use of spectral lines with different Landé factors has allowed determination of approximate correlations of magnetic and temperature images (Saar et al. 1994). However, the polarity of the field remains unclear, as does whether the field within the spots is more-or-less uniform, or is divided into small scale fields of opposite orientation. In the near future we may hope to obtain from spectropolarimetric observations information about the polarity distribution of such magnetic fields associated with these strong large scale nonaxisymmetric structures.

In the present paper we investigate the possibility of explaining such large scale fields in terms of mean field dynamo theory. Some sort of 'turbulent dynamo' is usually accepted as being responsible for the solar magnetic field and, by extension, a similar mechanism is believed to operate in other, chromospherically active, late type dwarfs with deep convection zones. Such a dynamo would then operate in the late type 'active giant' stars, such as mentioned above.

Nearly all detailed models of solar dynamos have adopted the 'mean field' approach (Krause & Rädler 1980). A quite general prediction from simple models of this sort, where the large scale velocity fields are chosen *a priori* to have a simple form (usually only differential rotation is present), is that axisymmetric mean fields are preferentially excited: in linear theory such fields are generally excited at lower dynamo numbers than nonaxisymmetric but, more importantly, axisymmetric fields are usually stable in the nonlinear regime. Rüdiger & Elstner (1994) have shown that including plausible anisotropies in the α-tensor results in lower critical dynamo numbers for nonaxisymmetric field generation than for axisymmetric, provided that the differential rotation is not too large. Further, Moss (unpublished) has shown that such solutions are stable when an α-quenching nonlinearity is included.

It is possible to choose simple but rather artificial distributions of differential rotation and alpha effect such that nonaxisymmetric fields are easier to excite and/or are nonlinearly

Send offprint requests to: David Moss

* The National Center for Atmospheric Research is sponsored by the National Science Foundation

stable (e.g. Rädler et al. 1990; Moss et al. 1991). In the presence of a sufficiently strong differential rotation there are clear magnetohydrodynamic reasons for this preference for axisymmetric field generation, associated with the winding up of the nonaxisymmetric field lines (Rädler 1986; Moss 1992). However the differential rotation in the interior of stars other than the sun is unknown. Further, we have no knowledge of the meridional circulation. A self consistent approach to stellar dynamos should determine the large scale velocity fields consistently and simultaneously with the large scale magnetic field: for example it is clear in general terms that magnetic fields will both drive a meridional circulation (that, *inter alia*, advects angular momentum) and act to reduce differential rotation (e.g. Moss 1992). The eventual state of the system will depend on the competition between the various dynamical processes. Simple models of mean field dynamos including incompressible hydrodynamics by Barker & Moss (1994) show that, contrary to previous experience, stable nonaxisymmetric magnetic fields can be found over a range of parameters without any 'tuning'. This result seems largely attributable to the latitudinal dependence of the differential rotation, together with the dynamically driven meridional circulation (both self-consistently determined). However, in these models the magnitude of the differential rotation is always small, it being driven solely by the azimuthal component of the Lorentz force.

To solve the global problem of turbulent compressible convection and magnetic field generation is, at present, impossible, although significant steps have been taken towards smaller scale simulations in box geometries that might be considered as models for processes occurring locally in turbulent convection zones (see, e.g., the review by Brandenburg 1994). In some earlier work, the global solar dynamo problem was tackled without introducing the α-effect parameterization, solving the full Navier-Stokes equations, but still parameterizing the smaller scales of the turbulence by introducing a scalar turbulent viscosity (e.g. Gilman & Miller 1981; Gilman 1983; Glatzmaier 1985; and references therein). These calculations were important, not least because they successfully demonstrated the existence of dynamo action, but they have failed so far to reproduce important features of the solar cycle.

An alternative, computationally less expensive, approach that allows an exploration of parameter space, whilst avoiding some of the arbitrary features of kinematic dynamo theory, is to use a parameterization of the turbulent Reynolds stresses. This concept is in some ways akin to the approach of mean field electrodynamics. In its most recent form it is known as the 'Λ-effect' (e.g. Rüdiger 1989 and references therein). This Λ-effect has already been included in dynamically consistent axisymmetric dynamo models (e.g. Brandenburg et al. 1991, 1992a). Further, a preliminary, quasi-kinematic investigation of the effects on the excitation of nonaxisymmetric magnetic fields of including such dynamics was reported by Barker & Moss (1993). They solved the purely hydrodynamical problem with a simple form for the parameterized Reynolds stresses (Λ-parameter $V^{(0)} = +1$, see Sect. 2), and used the resulting large scale velocity fields as input into a kinematic, nonaxisymmetric dynamo calculation, with a simple α-quenching nonlinearity. They did not attempt a comprehensive survey of parameter space, but for a moderately supercritical dynamo number and a Taylor number of 10^5 they found a stable nonaxisymmetric solution. For smaller Taylor numbers only axisymmetric solutions were stable. Differential rotation becomes stronger with increasing Taylor number and, for a Taylor number of 10^6, the increased differential rotation effectively discriminated against the nonaxisymmetric fields. In general terms, we can naively expect that these computations, ignoring any back reaction of the magnetic field on the fluid motions, will overestimate the role of the differential rotation at given Taylor number, although in practice the interactions are likely to be quite complex and hard to predict in detail.

We note that there have been a number of recent papers investigating the possibility that the *solar* dynamo operates at or just below the base of the convection zone (see, e.g., Durney et al. 1993; Rüdiger & Brandenburg 1994), although the question is certainly not yet resolved. For example, it may be that a 'distributed dynamo' operates through much of the convection zone, but that there is a turbulent pumping of magnetic flux downwards, towards the bottom of the convection zone (e.g. Kitchatinov 1991; Brandenburg et al. 1992b; Brandenburg 1994). Perhaps more relevantly in stars with very deep subsurface convection zones, the base of the convection zone/overshoot layer is geometrically of small relative volume, and it is not at all clear that the 'bottom dynamo' concept is appropriate for these stars. (It clearly does *not* apply to late type fully convective dwarfs!) Thus we adopt a conventional 'distributed dynamo' model in this paper.

We report the results of mean field dynamo calculations that include consistently the effects of the large scale incompressible dynamics with parameterized turbulent Reynolds stresses. This allows a driver for differential rotation to be present, whilst permitting competition between such turbulent angular momentum transport and the angular momentum transport by the magnetic stresses. Note that there is no longer any necessity to impose an α-quenching nonlinearity to limit the growth of the solutions at finite amplitude, as the Lorentz force feeds back directly on to the dynamics. The question of whether some form of α-quenching should be simultaneously considered is one that we bypass in this investigation.

We again find wide parameter ranges where nonaxisymmetric magnetic fields are the *only* stable solutions to the dynamo equations. We experienced difficulties (see Sect. 2) that prevented us from proceeding to Taylor numbers as large as we would have wished, and so were unable to verify directly our expectation that in general for strong enough differential rotation, stable nonaxisymmetric fields are not found. However we feel that this point is not really in doubt: the interesting result is that stable nonaxisymmetric magnetic fields are quite readily excited for intermediate values of the Taylor number.

2. The model

2.1. Equations

We solve the standard mean field dynamo equation

$$\partial \mathbf{B}/\partial t = \nabla \times (\mathbf{u} \times \mathbf{B} + \alpha \mathbf{B} - \eta_T \nabla \times \mathbf{B}), \quad (1)$$

and the modified Navier-Stokes equation

$$\rho \frac{Du_i}{Dt} = -\frac{\partial P}{\partial x_i} - \frac{\partial}{\partial x_j}(\rho Q_{ij}) + (\mathbf{j} \times \mathbf{B})_i, \quad (2)$$

in an incompressible fluid shell, $R_0 \leq r \leq R$ (r, θ, ϕ are spherical polar coordinates). In Eq. (1), $\mathbf{B}$ is the mean field, α is the conventional α-effect parameter and η_T is a turbulent resistivity. In Eq. (2), $\mathbf{j}$ is the current corresponding to $\mathbf{B}$, and the reduced pressure P includes the gravitational term.

$$Q_{ij} = D_{ij} - \nu_T(u_{i,j} + u_{j,i}) \quad (3)$$

is a parameterization of the turbulent Reynolds stresses in an incompressible fluid (e.g. Rüdiger 1989). The first term on the right hand side of (3) gives rise to a turbulent angular momentum transport and the second term represents a conventional turbulent diffusion, with eddy viscosity ν_T.

2.2. Λ and α effects

We adopt a simple model for the Λ-effect, with

$$D_{ij} = \begin{pmatrix} 0 & 0 & \Lambda_V \sin\theta \\ 0 & 0 & \Lambda_H \cos\theta \\ \Lambda_V \sin\theta & \Lambda_H \cos\theta & 0 \end{pmatrix} \Omega. \quad (4)$$

Following Rüdiger (1980) we write

$$\Lambda_V = \nu_T(V^{(0)} + V^{(1)} \sin^2\theta) f(r), \quad (5)$$

$$\Lambda_H = \nu_T H^{(1)} \sin^2\theta f(r), \quad (6)$$

where $V^{(0)}$, $V^{(1)}$ and $H^{(1)}$ are expected to be of order unity. See Rüdiger (1989) and Brandenburg et al. (1991, 1992a) for further details. We introduce for numerical convenience the factor $f(r)$, which is unity in $r > R_0 + 0.2R$ and goes smoothly to zero at R_0. The terms $V^{(1)}$ and $H^{(1)}$ become important for larger angular velocities, and should be included for the regime in which we are really interested. However we have restricted ourselves in these exploratory calculations to the case $V^{(1)} = H^{(1)} = 0$, in order to reduce the number of parameters (but see, e.g., Kitchatinov & Rüdiger (1993) who have recently given a relation between $H^{(1)}$, $V^{(1)}$ and $V^{(0)}$ for a certain turbulence model; also Tuominen & Rüdiger (1989)). We write $\alpha = \alpha_0 g(r) \cos\theta$, where α_0 is a constant and $g(r) = 1$ in $R_0 + 0.2 < r < R$ and goes smoothly to zero at $r = R_0$.

2.3. Boundary conditions

Boundary conditions are that the flow be stress free at $r = R$, and at $r = R_0$ if $R_0 > 0$. There is no radial flow at the boundaries. The magnetic field fits smoothly onto a vacuum field at $r = R$ and if $R_0 > 0$ the condition is that the region $r < R_0$ is a perfect conductor. If $R_0 = 0$, regularity conditions determine $\mathbf{u}$ and $\mathbf{B}$ there.

2.4. Numerical procedure

The magnetic and velocity fields can be written quite generally as

$$\mathbf{B} = \nabla \times (a\hat{\boldsymbol{\phi}}) + b\hat{\boldsymbol{\phi}} + \nabla \times \nabla \times (\Phi \hat{\mathbf{r}}) + \nabla \times (\Psi \hat{\mathbf{r}}), \quad (7)$$

$$\mathbf{u} = \nabla \times (\psi\hat{\boldsymbol{\phi}}) + v\hat{\boldsymbol{\phi}} + \nabla \times \nabla \times (S\hat{\mathbf{r}}) + \nabla \times (T\hat{\mathbf{r}}), \quad (8)$$

where a, b, v, ψ are independent of ϕ, and we put

$$\Phi(r,\theta,\phi) = \sum_{m=1}^{K} \Phi_m(r,\theta) e^{im\phi} \quad (9)$$

with similar modal expansions in ϕ for Ψ, S, T and the reduced pressure P. (We find it convenient to separate the axisymmetric and nonaxisymmetric parts.)

We use as scalings $x = r/R$, $\tau = (\eta_T/R^2)t$, $\mathbf{B}^* = R/(\eta_T^2 \rho \mu_0)^{1/2}\mathbf{B}$, $\mathbf{u}^* = (R/\eta_T)\mathbf{u}$ and $\alpha^* = R\alpha/\eta_T$. The nondimensional α-effect parameter is then $C_\alpha = \alpha_0 R/\eta_T$, and this is an input to the calculations. We take the magnetic Prandtl number ν_T/η_T to be unity. The other important input parameter is the Taylor number, $Ta = (2\Omega_0 R^2/\nu_T)^2$, where Ω_0 is the angular velocity of uniform rotation with the given angular momentum. Effectively, Ta specifies the (conserved) angular momentum. For diagnostic purposes it is useful to define

$$C_{\Omega,e} = [\Omega(R, \pi/2) - \Omega(R_0, \pi/2)]R^2/\eta_T, \quad (10)$$

and

$$C_{\Omega,g} = (\Omega_{\max} - \Omega_{\min})R^2/\eta_T. \quad (11)$$

Here $\Omega = u_{0\phi}/(r\sin\theta)$, with $u_{0\phi}$ the ϕ- independent azimuthal velocity. In (11), maximum and minimum values of Ω are taken either in the equatorial plane or globally. Note that in our model, C_Ω is not defined *a priori*, but emerges as part of the solution. $C_m = UR/\eta_T$, where U is the mean square meridional velocity (axisymmetric), is a magnetic Reynolds number for the meridional flow. We also define the global parity and symmetry parameters,

$$P = \frac{(E^{(S)} - E^{(A)})}{(E^{(S)} + E^{(A)})}, \quad (12)$$

$$M = 1 - \frac{E_0}{E}, \quad (13)$$

where E is the total magnetic energy, $E^{(S)}$ and $E^{(A)}$ are the parts corresponding to dynamo solutions symmetric and antisymmetric with respect to the rotational equator respectively, and E_0 is the energy in the axisymmetric part of the field. It is sometimes convenient to follow the evolution of solutions in a (P, M) diagram. The four 'corner solutions', with $(M, P) = (0, +1), (0, -1), (1, +1), (1, -1)$, can be associated with the nonlinear continuations of the linear modes S0, A0, S1, A1 respectively (e.g. Rädler et al. 1990), and thus we simply refer to them as such. There are so far no cases known where solutions with dominant $m = 2$ (or higher) modes are stable.

We integrate in time the $K+1$ modal components of equations derived from (1) and (2). The numerical procedure is described in more detail in Barker & Moss (1994). In addition to a modified Dufort-Frankel scheme, we here also used a second order Runge-Kutta method. The latter was slightly more robust, and was used at higher Taylor numbers. It is also necessary to solve Poisson type equations for the ϕ-component of the axisymmetric vorticity and the modal components of the reduced pressure, $P_m(r,\theta)$.

In general we found retaining just four Fourier modes to be adequate, in that the energy in modes with $m > 1$ rapidly becomes small (see also Table 2 in Rädler et al. 1990). For $Ta \leq 10^3$, a meridional spatial resolution of 21×41 grid points over $x_0 \leq x \leq 1$, $0 \leq \theta \leq \pi$ was satisfactory ($x_0 = R_0/R$). When $Ta \gtrsim 10^4$, higher meridional resolution was needed. This appears to be because of the formation of a boundary layer of Ekman type in the nonaxisymmetric part of the flow described by Eq. (2). This can be demonstrated as follows.

If δ is a radial scale of variation, from the pressure and diffusion terms in Eq. (2) we can make the order of magnitude estimate

$$\frac{R^2 P}{\delta} \sim \frac{\nu_T S}{\delta^2}. \tag{14}$$

After taking the divergence of Eq. (2), we can obtain also the estimate

$$P \sim \frac{\Omega S}{R}, \tag{15}$$

and so $\delta \sim \nu_T/(\Omega R)$, or $\delta/R \sim Ta^{-1/2}$.

We alleviated this problem by introducing a shell, $0.8 \leq x \leq 1$, in which the viscosity increased smoothly, to ca 10-fold its normal value at $x = 1$. We stress that this is a purely artificial device. This enhancement was only included in the nonaxisymmetric dynamics, and did not appear to affect significantly the dynamo solutions. Even this device, together with enhanced spatial resolution (to 61×61), was only sufficient to obtain solutions to $Ta = 5 \times 10^4$ in general, and to $Ta = 10^5$ for some restricted calculations. The finer spatial resolution (and smaller time steps) required make further computations prohibitively expensive.

Table 1. Values of $C_{\Omega,e}$ from a purely hydrodynamical model. The entries in parentheses for $Ta = 5 \times 10^4$ are interpolations from neighbouring values

	$V^{(0)}$		
Ta	-2	1	2
10^2	-64	4.9	6.7
10^4	-200	50	76
5×10^4	(-380)	(120)	(180)
10^5	-530	150	240
10^6	-1600	440	759

3. Background results for differential rotation

If the $m = 0$ azimuthal component of Eq. (2) only is solved, with a Λ-effect with $f(r) = 1$ and $V^{(1)} = H^{(1)} = 0$, the solution is

$$\Omega = A x^{V^{(0)}}, \tag{16}$$

where A is a constant determined by the prescribed total angular momentum, e.g. Rüdiger (1989). If the $m = 0$ meridional hydrodynamical equations are also solved simultaneously, a meridional circulation is introduced and $\Omega = \Omega(x,\theta)$, but the underlying solution (16) is still clearly apparent. (The kinetic energy in the meridional motions is no more than about 1% of that of the differential rotation.) In Table 1 we reproduce some results from Barker (1994) to illustrate the variation of C_Ω with Ta and $V^{(0)}$ for such solutions. (The differences between the values of Table 1 and those of Brandenburg et al. (1991) are largely due to the difference in shell thickness: the code used here is consistent with that of Brandenburg et al.) We note that the rotation law (16) with $|V^{(0)}| \gtrsim 1$, and also the hydrodynamical solutions summarized in Table 1, give an unrealistically large ratio of angular velocity at the surface and at the bottom of the thick shell. When the Lorentz forces are included (see below), this ratio is generally significantly reduced, but may still be considered rather large. However we adopted a standard value $V^{(0)} = +1$ for most of the calculations, in order to study solutions with a strong driver of differential rotation, in contrast to the work of Barker & Moss (1994) who took $V^{(0)} = 0$.

4. Results

We performed systematic sets of calculations with $V^{(0)} = +1$ for Taylor numbers of 10, 10^3 and 10^4. We also obtained limited results for $Ta = 5 \times 10^4$ and a single result, at reduced resolution, at Ta=10^5. When $Ta = 10^3$, most of the calculations were performed in the complete sphere, but some have $x_0 = 0.2$. Experiments suggest that this difference makes little quantitative and no qualitative difference, and the two cases are not distinguished in what follows. For other values of Ta and $V^{(0)} = +1$, our results are for the thick shell, $x_0 = 0.2$.

For $Ta \leq 10^4$, the results of Barker (1994) when $x_0 = 0.1$ show that $C_\alpha = 10$ is clearly supercritical for the A0, S0, A1 and S1 modes, and our results show that these critical C_α values do not change much when $x_0 = 0.2$. When $Ta > 10^4$, Barker showed that the A1 and S1 modes become progressively harder to excite as Ta increases. However at $Ta = 5 \times 10^4$ it can be estimated that $C_\alpha = 12$ is clearly supercritical for all the basic modes.

For $Ta \leq 10^4$ the A0 and S0 solutions are steady. When $Ta = 5 \times 10^4$ they are oscillatory. This, together with the increased values of C_Ω, suggest that the $\alpha\omega$ dynamo regime is just being reached at the largest Ta values for which our code could handle computations in which P and M were not restricted in value by boundary and initial conditions.

For orientation and interpretation of our results, note that the magnetic field strength for equipartition with the turbulent motions is given by

$$B_{\rm eq}^2 = \mu_0 \rho u_t^2. \tag{17}$$

In dimensionless form, with $\eta_T \sim \frac{1}{3}\ell u_t^2$, u_t and ℓ a typical turbulent velocity and length scale, this becomes

$$B_{\rm eq}^{*2} \sim 10(R/\ell)^2. \tag{18}$$

If $R \sim (3-10)\ell$, then $B_{\rm eq}^{*2} \sim 10^2 - 10^3$, and the dimensionless global equipartition magnetic energy $E_{mag,eq} \sim 20(R/\ell)^2 \sim 200 - 2000$.

In Sect. 4.1 to 4.4 we discuss our 'standard' case, $V^{(0)} = +1$. In Sects. 4.5 and 4.6 we briefly report assorted experiments with other values of $V^{(0)}$. For some of the calculations of Sect. 4.6, $x_0 = 0.0$.

4.1. $Ta = 10$

Taking $C_\alpha = 10$, we first computed the S0, A0, S1, A1 solutions: basic properties are given in Table 2. We then perturbed these solutions, both in global parity (P) and azimuthal symmetry (M), typically by less than 0.1% in each of these parameters, and followed the subsequent evolution of the system. We found the S1 solution to be stable, and the other three to be unstable. In particular, we followed the evolution of the configuration starting near $(M, P) = (0, -1)$ for a number of diffusion times. It at first evolved with $P \approx -1$ until M was very close to unity and then, at first very slowly, P began to increase with $M \approx 1$. In fact, when we perturbed the exact A1 solution, it moved away from the $(-1, 0)$ corner rather more rapidly than did the perturbed A0 configuration when at its closest to the A1 corner, as the distance of the latter from $P = -1$ was for a significant time smaller than the size of our standard perturbation in P.

Without rather extensive calculations it is difficult to be quite certain that other stable solutions do not exist, perhaps with quite small basins of attraction in (P, M) space. We did start one computation near the centre of the (P, M) diagram, with a fairly arbitrary initial field configuration. This evolved on a timescale of about a diffusion time to the $P = +1$, $M = 1$ state (see Fig. 1). Figure 2 gives angular velocity contours and meridional circulation streamlines for the S1 solution. With $C_\alpha = 12.5$, the evolution was qualitatively similar. A general feature of these and all the other solutions presented is that both the kinetic and magnetic energies are concentrated in the lowest order modes.

4.2. $Ta = 10^3$

The properties of the pure parity, 'corner' solutions are given in Table 2 for $C_\alpha = 10$. When these were perturbed, the results were quite similar to those with $Ta = 10$ and, again, the only stable solution was that with $P = +1$, $M = 1$. Evolution was, in general, somewhat more rapid. In particular, we followed the evolution of the perturbed A0 and A1 configurations for a number of diffusion times. The former also lingered near to the A1 corner for several diffusion times, as discussed above for $Ta = 10$, before evolving towards the stable S1 solution. Similarly, the perturbed A1 configuration was at first very slow to move away from $P = -1$: some details of its evolution are shown in Fig. 3. Again we did not find any other stable solution: for example a configuration starting near $P = 0.3$, $M = 0.4$, eventually evolved to $P = +1$, $M = 1$, after spending several diffusion times near $P = -1$, $M = 1$. Repeating the latter computation with C_α increased to 12.5 yielded similar results. We show surface magnetic field contours for $C_\alpha = 10$ and $P = M = 1$ in Fig. 4. (These contours are, in fact, quite typical of surface field contours for the S1 solutions for other values of Ta.)

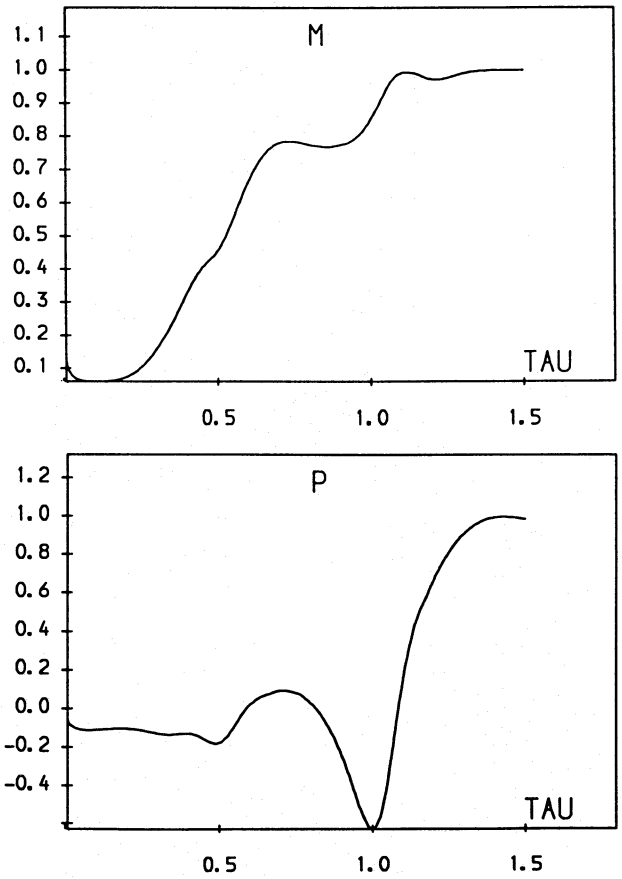

Fig. 1. Evolution in P and M at $Ta = 10$, $V^{(0)} = 1$, $C_\alpha = 10$ of configuration starting with $P \approx 0$, $M \approx 0.15$

4.3. $Ta = 10^4$

We first examined, at relatively low spatial resolution (21×41), the behaviour of solutions restricted to pure parity $P = +1$. (For reasons that we did not determine, these solutions were less demanding numerically than those with a $P = -1$ component). With $C_\alpha = 10$ we found limit cycle behaviour, with $0.97 \lesssim M \lesssim 0.99$. With $C_\alpha = 12, 14$ the corresponding variations were $0.73 \lesssim M \lesssim 0.94$ and $0.81 \lesssim M \lesssim 0.95$ respectively. We give some details of the $C_\alpha = 12$ solution in Fig. 5. A

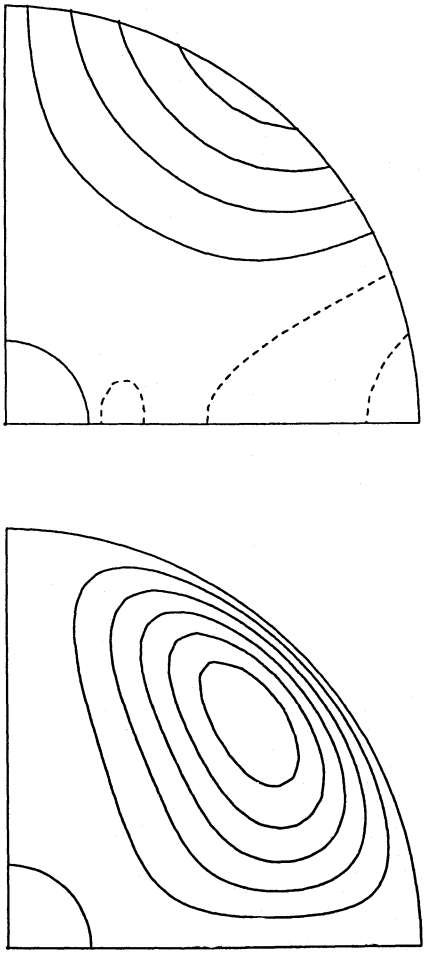

Fig. 2. Equally spaced contours of constant angular velocity and meridional circulation streamlines for S1 solution, $Ta = 10$, $V^{(0)} = 1$, $C_\alpha = 10$

test run at resolution 61×61 suggested that these limits changed somewhat, but that the limit cycle character of the solution remained. When $C_\alpha = 12$ we verified that the limit cycle was unstable to perturbations in P.

Turning now to the pure parity solutions, the A0 solution was found to be stable to small perturbations in M and P with $C_\alpha = 10$, and the other pure parity solutions were unstable. The S1 solution is stable when perturbed in P alone – see also Sect. 4.5 and the discussion in Sect. 5. Details of these basic solutions are again given in Table 2. For the A0 solution with $C_\alpha = 10$, we show angular velocity contours and circulation streamlines in Fig. 6.

4.4. $Ta = 5 \times 10^4$

Because of numerical problems/large cpu requirements, we were only able to make a limited investigation of this case. With $C_\alpha = 10$, from the results of Barker (1994) it can be deduced that the pure parity modes are, at best, only marginally excited. Thus we took $C_\alpha = 12$, when we found *all* the pure parity solutions to be unstable to arbitrary perturbations. When the solutions were restricted to be axisymmetric, then the A0 solution was stable. When the parity was restricted to $P = +1$ (at low resolution and still with $C_\alpha = 12$), we again found limit cycle behaviour, with $0.93 \lesssim M \lesssim 0.99$, whereas when $C_\alpha = 11$ and $P = +1$, the eventual state is $M = 1$.

Table 2. Results for the saturated pure parity modes with $V^{(0)} = 1$. $C_\alpha = 10$, except for $Ta \geq 5 \times 10^4$, where $C_\alpha = 12$. A few C_m values were not calculated, but there is no reason to expect them to differ very much from those given. Oscillatory solutions are denoted by asterisks. In these cases the energy values are means of the maximum and minimum values in the oscillation (which may be markedly non-sinusoidal), whereas the $C_{\Omega,g}$, $C_{\Omega,e}$ and C_m entries are merely typical values. Kinetic energies are in the inertial frame and include the kinetic energy of solid body rotation at angular velocity Ω_0, which is $\pi Ta/15$. In the last column, Ω_s/Ω_i is the ratio in the equatorial plane of the angular velocity at the surface to that at $x = 0.2$. Stable solutions are shown in bold face

Ta	mode	$E_{\rm mag}$	$E_{\rm kin}$	$C_{\Omega,g}$	$C_{\Omega,e}$	C_m	Ω_s/Ω_i
10	A0	235	71	86	−27	1.3	0.2
	S0	335	96	66	−0.8	3.1	−0.9
	A1	447	120	59	21		0.04
	S1	614	180	56	1		1.0
10^3	A0	238	274	87	−11	0.7	0.7
	S0	227	286	74	22		0.9
	A1	407	293	54	28		1.6
	S1	651	364	67	21	2.9	−1.2
10^4	**A0**	301	2200	115	20	1.1	1.4
	S0	136	2170	89	62	1.0	2.3
	A1	481	2130	54	47	1.8	3.7
	S1	1140	2180	56	27	3.5	1.9
5×10^4	A0*	610	10800	180	84	1.4	2.4
	S0*	1770	11200	200	74	1.7	2.1
	A1	2090	10600	79	43	4.2	1.5
	S1	4540	12300	129	46	5.3	1.6
10^5	S1	3200	24600	102	65	4.7	1.6

Table 3. Some results for the saturated pure parity modes with $V^{(0)} = 0.3$, $C_\alpha = 10$ (12 when $Ta = 10^5$). Details as in Table 2

Ta	mode	$E_{\rm mag}$	$E_{\rm kin}$	$C_{\Omega,g}$	$C_{\Omega,e}$	C_m
10^3	S1	701	367	56	10	2.8
10^4	A0	310	2170	103	5	1.4
	S0	283	2120	103	7	
	S1	957	2240	57	25	3.4
10^5	S1	3460	21200	98	37	4.3

4.5. $V^{(0)} = 0.3$

We made a limited investigation of the case $V^{(0)} = 0.3$ for $Ta = 10^3$ to 10^5. Results for the pure parity modes are given in Table 3. For $C_\alpha = 10$, the S1 solution is stable to an arbitrary perturbation when $Ta = 10^3$. When $Ta = 10^4$, the S1 solution is unstable (in contrast to the situation when $V^{(0)} = 0$, cf. also Barker & Moss 1994), but the instability develops very slowly. In this case, the A0, S0 and A1 solutions are also unstable: in particular we found that the perturbed A0 solution evolved

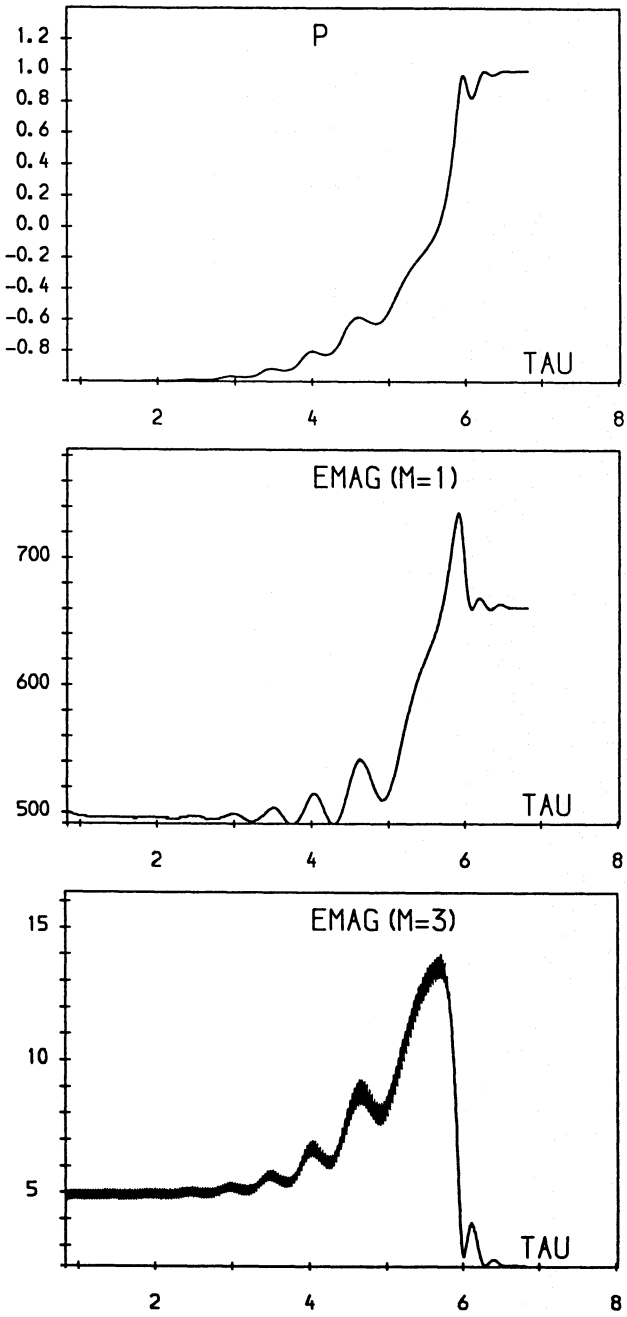

Fig. 3. Evolution in time of P and the energies of the $m = 1$ and $m = 3$ parts of the magnetic field for the perturbed A1 case: $Ta = 10^3$, $V^{(0)} = 1$, $C_\alpha = 10$. The energies in the $m = 0, 2$ parts of the field are always small

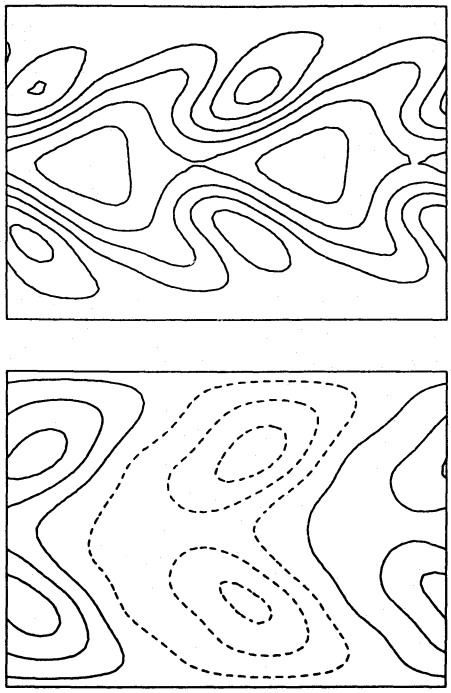

Fig. 4. Equally spaced contours of total field strength $|\mathbf{B}|$ (top) and radial field B_r (bottom) for S1 solution at one grid point beneath the surface, $Ta = 10^3$, $V^{(0)} = 1$, $C_\alpha = 10$. Longitude $(0, 2\pi)$ runs from left to right, latitude $(0, \pi)$ from top to bottom. Broken contours represent negative values. Maximum values of total field strength occur at mid-latitudes, and are of order $5(\ell/R)B_{\rm eq}$

rapidly, at first to near $P = -1$, $M = 1$ and then, with M keeping very close to unity, to the S1 configuration. This is in apparent contradiction to the finding that the S1 solution is unstable: the resolution of the situation appears to be that the basin of attraction of the S1 solution contains a very narrow wedge with $M \approx 1$ near $P = +1$: our arbitrary, but small, perturbation took the solution outside of this wedge. When $Ta = 10^5$, $C_\alpha = 12$, the S1 solution is stable to an arbitrary perturbation, but weakly in the sense that the return to $P = M = 1$ is relatively slow.

4.6. Other values of $V^{(0)}$

Starting from arbitrary field configurations near the middle of the (P, M) diagram, we found evolution to $P = +1$, $M = 1$ in the following cases. $Ta = 10^2$: $C_\alpha = 10$, $V^{(0)} = +2$ and -1. $Ta = 10^3$: $C_\alpha = 10$, $V^{(0)} = +3$ and $+2$. We made only short runs with other parameters, that were insufficient to determine the final state; in no case did we find evidence for evolution to any state other than $P = +1$, $M = 1$ with $Ta \leq 10^3$. However when $Ta = 10^3$, $V^{(0)} = -2$, $C_\alpha = 10$, the system again closely approaches $P = -1$, $M = 1$ from arbitrary initial conditions, and was extremely slow to move away. However it seemed clear (Fig. 7) that the eventual state is not the A1 solution, although we did not run this case long enough to determine the final configuration: from comparison with the corresponding calculation with $V^{(0)} = +1$ it is plausible that the eventual state is again S1. When $Ta = 5 \times 10^4$, $V^{(0)} = -2$, Barker (1993) showed that the $m = 1$ modes are much harder to excite than those with $m = 0$ and that the S0 mode is significantly easier to excite than the A0 with these parameters. In this case, when $C_\alpha = 10$ an arbitrary initial field configuration unsurprisingly evolves to the S0 solution.

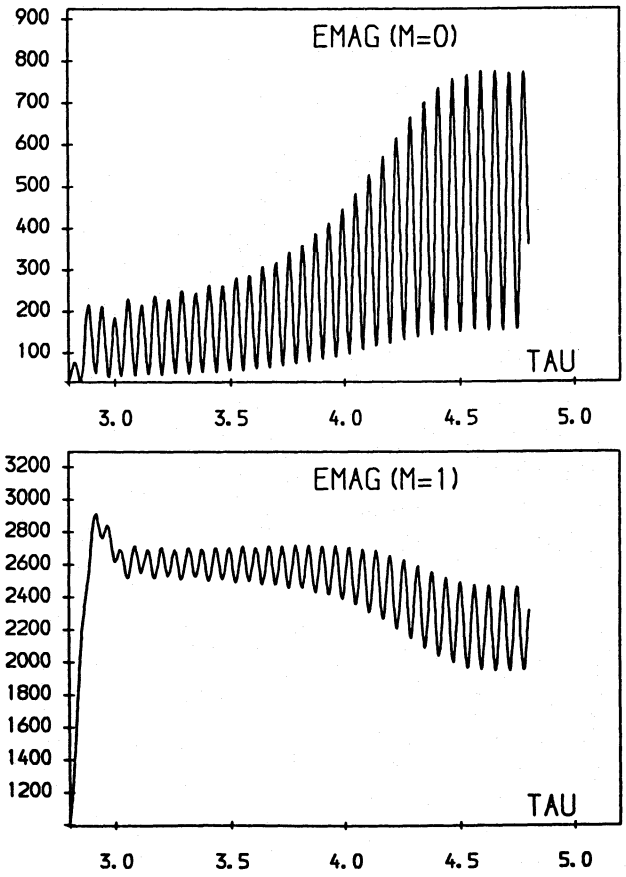

Fig. 5. $m = 0$ and $m = 1$ magnetic and kinetic energies during the approach to the limit cycle for the $Ta = 10^4$, $V^{(0)} = 1$, $C_\alpha = 12$ solutions with the restriction $P = +1$

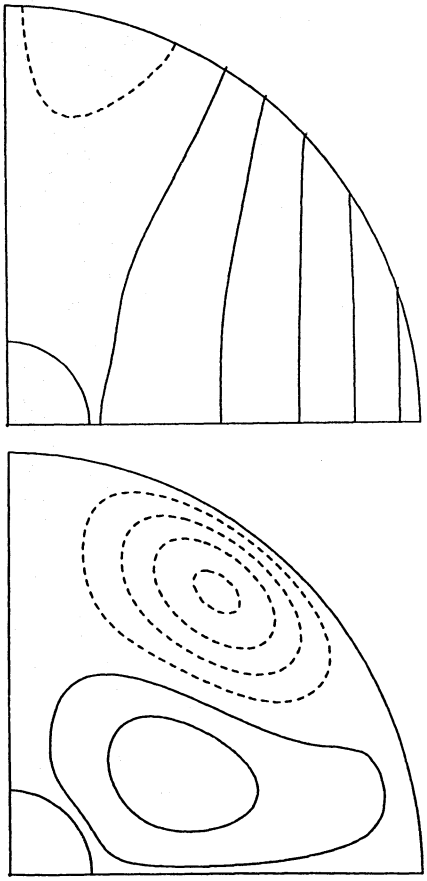

Fig. 6. Equally spaced contours of constant angular velocity and meridional circulation streamlines for A0 solution, $Ta = 10^4$, $V^{(0)} = 1$, $C_\alpha = 10$

5. Discussion

Our principal result is that, in a model where the large scale velocity fields are determined consistently with the magnetic field, stable nonaxisymmetric magnetic fields can be excited at moderate values of the Taylor number for a range of values of the Reynolds stress parameter $V^{(0)}$. These fields are of S1 type – i.e. of the same general topology as a 'perpendicular dipole'. The results seem to be insensitive to Taylor number for $10 \leq Ta \leq 10^3$, and also not to depend strongly on $V^{(0)}$ for these values. The controlling factor seems to be the magnitude of the differential rotation, but inspection of Table 1 shows that, for $Ta \lesssim 10^4$, the absolute differential rotation $|C_\Omega|$ is small for all values of $V^{(0)}$. However, Barker & Moss (1994) found the S1 solution to be stable at $Ta = 10^4$ with $V^{(0)} = 0$, in contrast to our results with $V^{(0)} = 0.3$ and 1. This suggests that in transitional regimes stability properties may be sensitive to model parameters. We note that the magnetic energy of the S1 solution is always by far the largest among the pure modes for given Ta and $V^{(0)}$ (see Table 2); the significance of this result is unclear. We were unable to calculate self-consistent nonaxisymmetric models for Taylor numbers larger than a few times 10^4. Table 1 confirms that it is in this regime that $|C_\Omega|$ generally attains values of a few hundreds, where the $\alpha\omega$ regime of kinematic dynamo models is approached. This is confirmed by our axisymmetric solutions being steady for $Ta \leq 10^4$ and oscillatory at 5×10^4 when $V^{(0)} = 1$. We were also restricted to only mildly supercritical values of C_α. In the range investigated, results do not appear to be very dependent on C_α, provided that the basic dynamo modes are all excited. Nevertheless, previous experience with kinematic dynamos, and with axisymmetric hydrodynamical dynamos, does suggest that some results might depend to an extent on the value of C_α: naively, larger C_α might produce stronger fields and hence more effective Lorentz torques and so smaller $|C_\Omega|$.

We note the interesting situation found with the $V^{(0)} = 0.3$, $Ta = 10^4$ solutions. A configuration initially far from the S1 corner of the (P, M) diagram evolves to S1, approaching this solution along the line $M = 1$. However the S1 solution is unstable to an arbitrary perturbation in P and M, and evolves with P and M decreasing (we did not follow this evolution very far, as it was extremely slow.) Thus any evolution to S1 will be followed by movement away from it, if there is a finite perturbation in M. (A somewhat similar situation may have been encountered by Rädler et al. (1990) with a kinematic model, but their computation does not seem to have been continued for long enough for the outcome to be certain. *Inter alia*, they

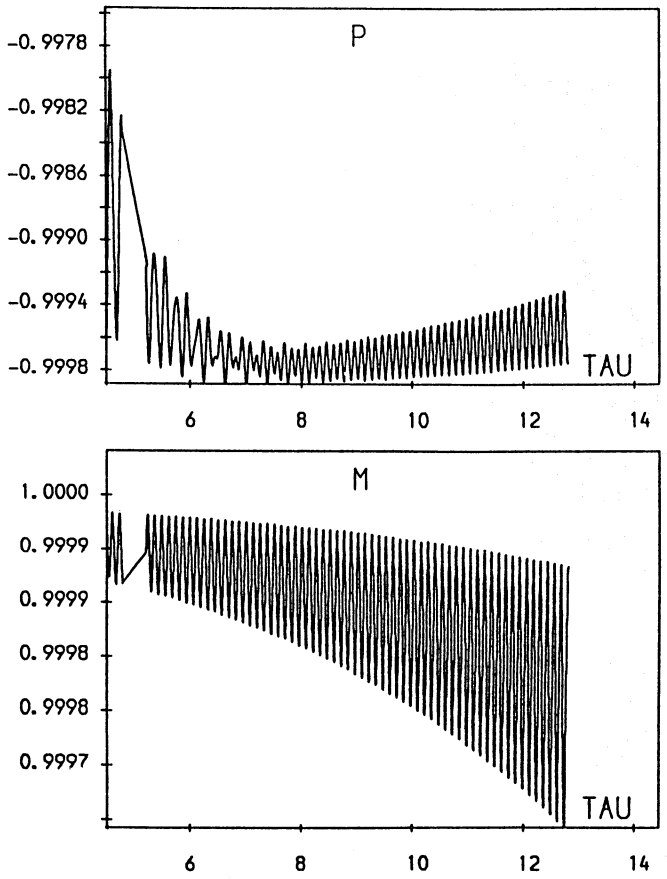

Fig. 7. Part of the evolution in P and M of a run starting with $P \approx 0$, $M \approx 0.35$, showing the approach to and slow divergence from $P = -1$, $M = 1$. $Ta = 10^3$, $V^{(0)} = -2$, $C_\alpha = 10$. The anomalies at $\tau \approx 5$ are caused by some data having been lost

pointed out that the evolution through the (P, M) plane can take hundreds of (turbulent) magnetic diffusion times (see also Barker & Moss 1994).) There is no completely stable solution available for these parameters, and it seems plausible that the system will eventually again be captured by S1, approaching along $M = 1$. Thus an irregular cycling may result, if any noise is present. Although we did not investigate the corresponding $V^{(0)} = 1, Ta = 10^4$ case in so much detail, the results of Sect. 4.3 suggest a somewhat similar situation, except that the A0 solution is now stable. We can speculate that the $V^{(0)} = 1, Ta = 5 \times 10^4$ case may also be similar.

In fact, the argument against the existence of strictly non-axisymmetric solutions for large Taylor numbers (differential rotation) is simple: as soon as the differential rotation becomes large enough ($|C_\Omega|$ typically a few hundreds), the critical C_α values for nonaxisymmetric modes increase to values significantly larger than for the axisymmetric modes. (Magnetic torques will oppose the growth of $|C_\Omega|$, but it is probable that the hydrodynamical effects will eventually dominate; cf. also Moss 1992.) Thus there is a range of C_α values for which the only pure parity modes that can be excited are axisymmetric. If C_α is very supercritical for these modes, then $m > 0$ modes can be excited, but there is no evidence that such solutions would be stable, unless perhaps the dynamo operates in a regime well past this bifurcation (cf. Jennings 1991). Likewise there is no numerical evidence to date for the existence of mixed $m = 0$ and $m > 0$ solutions existing in a regime where only $m = 0$ modes are excited in linear theory. This, together with the general argument by Rädler (1986), many kinematic results and the quasi-kinematic calculations of Barker & Moss (1993), suggests strongly that for larger Taylor numbers and, correspondingly, differential rotation, only axisymmetric solutions are stable. By this reasoning, the reversion to a stable axisymmetric solution at $Ta = 10^4$, $V^{(0)} = +1$, would appear to owe more to the changing spatial structure of Ω (see below) than to the magnitude of the differential rotation. It is unclear how the situation at $Ta = 5 \times 10^4$ fits into this picture, and there are clearly other important effects that influence stability in intermediate regimes.

It is interesting to assess the importance of the azimuthal restoring torques, by comparing the $C_{\Omega,e}$ values of Table 2 with the C_Ω entries in Table 1, remembering that in the models of Barker & Moss (1994) a C_Ω value of about 50 can be generated by the action of the Lorentz force alone, and so for $Ta \lesssim 10^3$ the differential rotation (Table 2) is predominantly driven by the Lorentz force. For $Ta \geq O(10^4)$ there is a small but clear reduction. A similar conclusion follows from inspection of the relative differential rotation in the last column of Table 2.

We note that for $Ta = 10$, differential rotation contours for the S1 solution are 'disc-like' (Fig. 2), whereas for $Ta \gtrsim 10^4$, Ω is almost constant on cylinders (Fig. 6). Comparison of the Ω contours at $Ta = 5 \times 10^4$ for the S0 and S1 solutions shows that $\Omega \approx \Omega(z)$ is perhaps rather more effectively enforced in the S1 solution. In general, Lorentz torques seem slightly more effective at controlling differential rotation when $m = 1$, compared to when $m = 0$.

We distinguish between the *absolute* differential rotation parameter C_Ω, which is important for dynamo theory, and the relative rotation Ω_s/Ω_i. Whereas $|C_\Omega|$ is never very large in our models, a somewhat unrealistic feature of some of our solutions, if we want to apply them to real stars, is the relatively large value of Ω_s/Ω_i. Also, there are even some negative values! The latter seem to arise since, for smaller values of Ta, the azimuthal velocities produced by the Lorentz forces are comparable to those from the Λ-effect. Moreover our choice of Λ-profile, with $\Lambda \to 0$ at the base of the envelope, means that the Reynolds stresses are ineffective there and so the Lorentz stresses dominate locally. For comparison, the underlying rotation solution (16) gives $\Omega_s/\Omega_i = 5$ for $V^{(0)} = 1$ – the marked deviations from this value (Table 2) are a measure of the effectiveness of angular momentum transport by meridional flows and Lorentz stresses. (For $V^{(0)} = 0.3$ the corresponding 'background' value of Ω_s/Ω_i is 1.6.)

In general, we are encouraged that overall our results appear not to be very sensitive to the value of $V^{(0)}$. Indeed, our results differ in detail, but not in substance, from those of Barker & Moss (1994). In that paper, $V^{(0)} = 0$, and there was thus no external driver for the differential rotation. This also means that the large values of Ω_s/Ω_i of some of our models (see above)

are not crucial to the existence of stable nonaxisymmetric solutions. As previously noted, our choice of Λ parameter is strictly appropriate only to relatively slow rotation. A more extensive investigation would certainly include non-zero values of $V^{(1)}$ and $H^{(1)}$ (Eqs. (5) and (6)). However, given all the uncertainties of detail associated with the model, we feel that such elaboration at the moment would be premature.

We have completely neglected any micro-feedbacks on to the dynamics (e.g. α-quenching, buoyancy, Λ-quenching) or turbulent diamagnetic effects, all of which have recently been discussed. It would be important to assess their relative importance (see recent work by Kitchatinov & Rüdiger 1993), but here we have chosen to isolate the effects of the large scale feedback from the Lorentz force. It is plausible that any Λ-quenching might, by reducing the effective value of Λ, reduce the absolute differential rotation for given $V^{(0)}$ – see the above discussion. (Note that the calculations reported in Barker & Moss (1993) could be considered to apply to the limit of a dominant α-quenching, that is effective at field strengths below those at which the Lorentz force has a significant effect on the large scale dynamics.) Likewise we have neglected possible anisotropies in the α-coefficient and in the turbulent resistivity and viscosity.

6. Concluding remarks

We have shown that stable nonaxisymmetric magnetic fields may quite naturally be excited in deep convective shells. We recognise that our solutions do not directly suggest the presence of *equatorial* spots, such as are indicated by surface imaging techniques (Piskunov et al. 1990, 1994), but rather spots at mid-latitudes (Fig. 4; cf. also Moss et al. 1991). Certainly the situation in these stars is rather more complex than anything produced by our models: the 'flip-flop' phenomenon, reported in several stars (e.g. Jetsu et al. 1993, 1994) is particularly intriguing. Nonetheless we feel that our models may be capturing, in a very simple way, the essence of the field generation process in these stars.

There is some observational evidence that latitudinal differential rotation on the surfaces of late type giant stars is small, i.e. $|\Delta\Omega/\Omega| \ll 1$. There is also some evidence (e.g. Hall 1991) that the differential rotation is smaller for active than for non-active giant stars. On the sun, the surface differential rotation is much larger, and it is there associated with a radial differential rotation of comparable magnitude. If such a comparison is valid, then this may be evidence for relatively weak radial differential rotation in late type active giant stars, that is for conditions favourable for nonaxisymmetric field generation.

Acknowledgements. This work was supported by SERC Grant GR/F77494. DMB, AB and DM are grateful for the hospitality of the University of Helsinki Observatory.

References

Barker, D. M.: 1993, In Theory of Solar and Planetary Dynamos (ed. P.C. Matthews & A.M. Rucklidge), Cambridge University Press p.27

Barker, D. M. & Moss, D.: 1993, In The Cosmic Dynamo (ed. F. Krause, K.-H. Rädler & G. Rüdiger), Kluwer Acad. Publ., Dordrecht p.147

Barker, D. M. & Moss, D.: 1994, A&A 283, 1009

Brandenburg, A.: 1994, In Lectures on Solar and Planetary Dynamos (ed. M. R. E. Proctor & A. D. Gilbert), Cambridge University Press

Brandenburg, A., Moss, D., Rüdiger, G., Tuominen, I.: 1991, Geophys. Astrophys. Fluid Dyn. 61, 179

Brandenburg, A., Moss, D., Tuominen, I.: 1992a, A&A 265, 328

Brandenburg, A., Moss, D., Tuominen, I.: 1992b, In The Solar Cycle (ed. K. L. Harvey), ASP Conference Series, 27 p.536

Durney, B. R., De Young, D. S., Roxburgh, I. W.: 1993, Solar Phys. 145, 207

Hall, D. S.: 1991, In The Sun and cool stars: activity, magnetism, dynamos (ed. I. Tuominen, D. Moss & G. Rüdiger), Lecture Notes in Physics 380, Springer-Verlag p.353

Jennings, R. L.: 1991, Geophys. Astrophys. Fluid Dyn. 57, 147

Jetsu, L.: 1993, A&A 276, 345

Jetsu, L., Pelt, J., Tuominen, I.: 1993, A&A 278, 449

Jetsu, L., Tuominen, I., Grankin, K. I., Mel'nikov, S. Yu., Shevchenko, V. S.: 1994, A&A 282, L9

Gilman, P. A.: 1983, ApJS 53, 243

Gilman, P. A., Miller, J.: 1981, ApJS 46, 211

Glatzmaier, G. A.: 1985, ApJ 291, 300

Kitchatinov, L. L.: 1991, A&A 243, 483

Kitchatinov, L. L., Rüdiger, G.: 1993, A&A 276, 96

Krause, F., Rädler, K.-H.: 1980, Mean-Field Magnetohydrodynamics and Dynamo Theory. Akademie-Verlag, Berlin; also Pergamon Press, Oxford

Moss, D.: 1992, MNRAS 257, 593

Moss, D., Tuominen, I., Brandenburg, A.: 1991, A&A 245, 129

Piskunov, N. E., Tuominen, I., Vilhu, O.: 1990, A&A 230, 363

Piskunov, N. E., Huenemoerder, D. P., Saar, S.H.: 1994, In Eighth Cambridge Workshop on Cool Stars, Stellar Systems, and the Sun (ed. J.-P. Caillault), Astron. Soc. Pac. Conf. Ser., Vol.

Rädler, K.-H.: 1986, Plasma Physics ESA SP-251, 569

Rädler, K.-H., Wiedemann, E., Brandenburg, A., Meinel, R., Tuominen, I.: 1990, A&A 239, 413

Rüdiger, G.: 1980, Geophys. Astrophys. Fluid Dyn. 16, 239

Rüdiger, G.: 1989, Differential rotation and stellar convection: Sun and solar-type stars. Gordon & Breach, New York

Rüdiger, G. & Brandenburg, A.: 1994, A&A (submitted) A solar dynamo in the overshoot layer: cycle period and butterfly diagram

Rüdiger, G. & Elstner, D.: 1994, A&A 281, 46

Rüdiger, G., Kitchatinov, L. L.: 1990, A&A 236, 503

Saar, S.H., Piskunov, N.E., Tuominen, I.: 1994, In Eighth Cambridge Workshop on Cool Stars, Stellar Systems, and the Sun (ed. J.-P. Caillault), Astron. Soc. Pac. Conf. Ser., Vol.

Tuominen, I., Rüdiger, G.: 1989, A&A 217, 217

This article was processed by the author using Springer-Verlag LaTeX A&A style file *L-AA* version 3.